

Chaotic motion in multi-black hole spacetimes and holographic screens

William Hanan and Eugen Radu

Department of Mathematical Physics, National University of Ireland, Maynooth, Ireland

March 24, 2022

Abstract

We investigate the geodesic motion in D -dimensional Majumdar-Papapetrou multi-black hole spacetimes and find that the qualitative features of the $D = 4$ case are shared by the higher dimensional configurations. The motion of timelike and null particles is chaotic, the phase space being divided into basins of attraction which are separated by a fractal boundary, with a fractal dimension d_B . The mapping of the geodesic trajectories on a screen placed in the asymptotic region is also investigated. We find that the fractal properties of the phase space induces a fractal structure on the holographic screen, with a fractal dimension $d_B - 1$.

Introduction— The notion of chaos is one of the most important ideas to explain various nonlinear phenomena in nature. An interesting case in which deterministic chaos may occur is given by the geodesic motion in general relativity. The nonlinearity of Einstein's equations may give rise to chaos in systems whose Newtonian analogue is nonchaotic. Relativistic systems in which chaos is known to appear include charged particles in a magnetic field interacting with gravitational waves [1], particles near a black hole in a Melvin magnetic universe [2], or in a perturbed Schwarzschild spacetime [3], [4] (see [5] for a general discussion and other examples).

The geodesic motion in a Majumdar-Papapetrou (MP) multi-black hole spacetime [6, 7] provides another particularly interesting situation. The MP spacetime is a solution of the Einstein-Maxwell system in D -dimensions, describing a collection of N extremal black holes located at random in a $D-1$ dimensional hypersurface. Each black hole has an electric charge equal to its mass, the gravitational and electrostatic forces canceling pairwise. As found by several authors [8], [9], [10], the motion of particles for $N = 2, 3$ MP black holes in four dimensions is chaotic, the phase space being divided into basins of attraction which are separated by a fractal boundary.

In recent years there has been a great deal of attention devoted towards research in black hole physics in higher dimensions, these exhibiting a number of new properties as compared to the $D = 4$ case.

The main purpose of this paper is to examine how the chaotic geodesic motion in a MP multi-black hole background depends on the spacetime dimensionality.

In this context, we consider the mapping of the geodesic trajectories onto a planar screen placed at a large distance from the black holes. We find that the fractal properties of the phase space induces a fractal structure on the holographic screen.

Chaotic motion in MP spacetime— The MP solution in a D -dimensional spacetime has a line element

$$ds^2 = -U^{-2}dt^2 + U^{\frac{2}{D-3}} \left((dx^1)^2 + \dots + (dx^{D-1})^2 \right), \quad (1)$$

where U is a function of x^μ satisfying the Laplace equations in a $D-1$ dimensional Euclidean space

$$U = 1 + \sum_{i=1}^N \frac{M_i}{|r - r_i|^{D-3}}, \quad (2)$$

and describes a system of extreme black holes in Einstein-Maxwell theory with equal charges and masses $M_i > 0$. Here $|r - r_i|$ denotes the Euclidean distance between the field point r and the fixed location r_i in a Euclidean space: $|r - r_i| = (\sum_{\mu=1}^{D-1} (x^\mu - x_i^\mu)^2)^{1/2}$. The black hole locations, r_i , are arbitrary, the event horizon area of a black hole being $M_i A_{D-2}$, where A_{D-2} is the area of a unit sphere in $D-2$ dimensions. The Maxwell one-form is given by $\mathcal{A} = U \sqrt{(D-2)/(2(D-3))} dt$. Note that this solution is static, with $\partial/\partial t$ a Killing vector, but in general it has no other symmetries.

Restricting ourselves to the case of an uncharged test particle and considering the contravariant components (γ, \mathbf{u}) of the velocity in an orthonormal basis, the geodesic equations of motion are given by

$$\dot{\mathbf{x}} = U^{-1/(D-3)} \mathbf{u}, \quad \dot{t} = U\gamma, \quad \gamma = \sqrt{\epsilon + u^2}, \quad (3)$$

$$\dot{\mathbf{u}} = U^{-\frac{D-2}{D-3}} \left[(\gamma^2 + \frac{1}{D-3} u^2) \nabla U - \frac{1}{D-3} \mathbf{u} \mathbf{u} \cdot \nabla U \right], \quad (4)$$

where $\epsilon = 0, 1$ for null and timelike particles respectively; an overdot indicates the derivative with respect to τ , which is an affine parameter along the geodesics (τ is the proper time for $\epsilon = 1$). These equations are supplemented with suitable boundary conditions, $\mathbf{x}(\tau_0) = \mathbf{x}^{(0)}$, $\mathbf{u}(\tau_0) = \mathbf{u}^{(0)}$, and possess a first integral associated with the Killing vector $\partial/\partial t$.

The geodesic equations have been integrated by using a standard differential equation solver for spacetime dimensions between four and eight. To simplify the general picture, the black holes were taken to have equal masses $M_i = M$, and were placed equidistantly along the x^2 -axis. The geodesic motion was considered mainly in the (x^1, x^2) plane only, *i.e.* $x^\mu = 0$, for $\mu > 2$. Special attention has been paid to the case $D = 5$. For $D = 4$, our results are in very good agreement with those in [9, 10].

The trajectories are evolved numerically until an outcome is reached. For a two black hole system, we distinguish three possible outcomes: a test particle may reach the first black hole, the second black hole or may orbit indefinitely.

This last possibility has two different subclasses: there are particles which escape to infinity and particles that get confined and follow indefinitely an orbit in a limited region

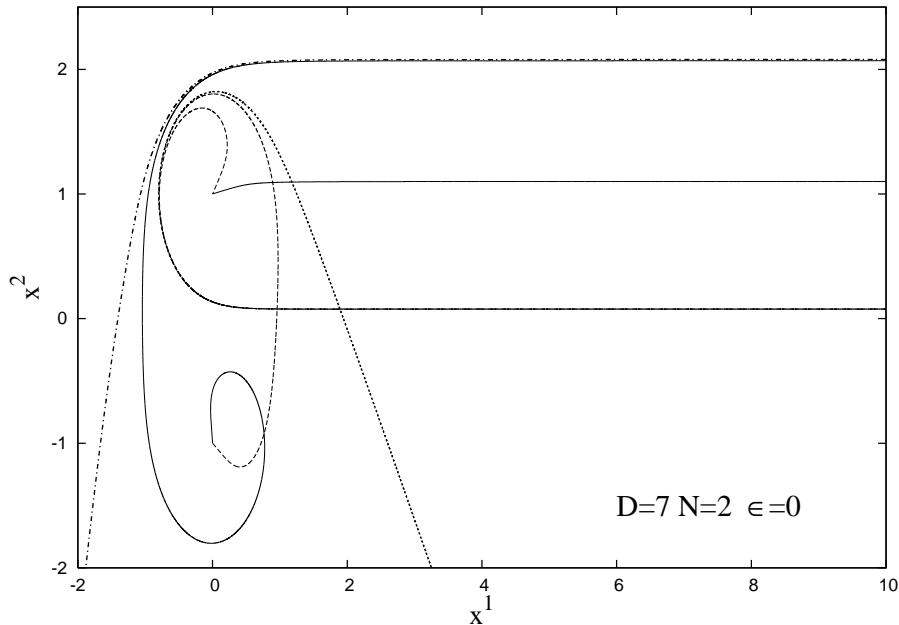


Figure 1. Typical null trajectories are shown for a $D = 7$, $N = 2$ MP black hole. The black holes are located on the x^2 -axis, at $+1$ and -1 respectively. The test particles start at $x^1(0) = 10$ with $u_i^{(0)} = -10\delta_i^1$.

of spacetime. Typical null trajectories illustrating these outcomes are shown in Figure 1 for a $D = 7$, $N = 2$ system, the orbits of massive particles presenting a rather similar shape.

A $\mathbf{u}^{(0)} = 0$ slice of phase space for $D = 5$, $N = 2$ timelike test particles is presented in Figure 2. The two black holes there have equal masses $M_i = 0.01$ and are placed at $(0, -1)$ and $(0, 1)$ respectively. The initial location of the test particle is painted black if it ends at $(0, -1)$ and white if it hits the second black hole at $(0, 1)$.

One can see that these pictures look similar to those exhibited in the literature for the $D = 4$ case [9, 10]. In particular, the boundary between the basins of attraction clearly has a complicated structure, which may be quantified using the concept of fractal dimension (see [10, 11] for other possible approaches).

To estimate the fractal dimension of the basin boundary we use the definition

$$d_B = \lim_{\varepsilon \rightarrow 0} \frac{\ln N(\varepsilon)}{\ln(1/\varepsilon)}, \quad (5)$$

where $N(\varepsilon)$ is the minimal number of boxes of size ε needed to cover the fractal set. In practice one estimates d_B by plotting $\ln N(\varepsilon)$ vs. $\ln \varepsilon$. The value of d_B evaluated for the data in Figure 2 on a grid with 2500^2 points is $d_B = 1.34 \pm 0.07$. This noninteger value shows in a coordinate invariant way that the basin boundary is indeed a fractal.

A qualitatively similar picture was found for all configurations we have considered, *i.e.* we did not notice the existence of a critical spacetime dimension, beyond which, for example, the structure cease to be fractal in nature. However, our findings indicate that, for a given (D, N) , the fractal dimension is configuration dependent, even for $\mathbf{u}^{(0)} = 0$. That is, changing the mass parameter or the location of the black holes leads to different values of

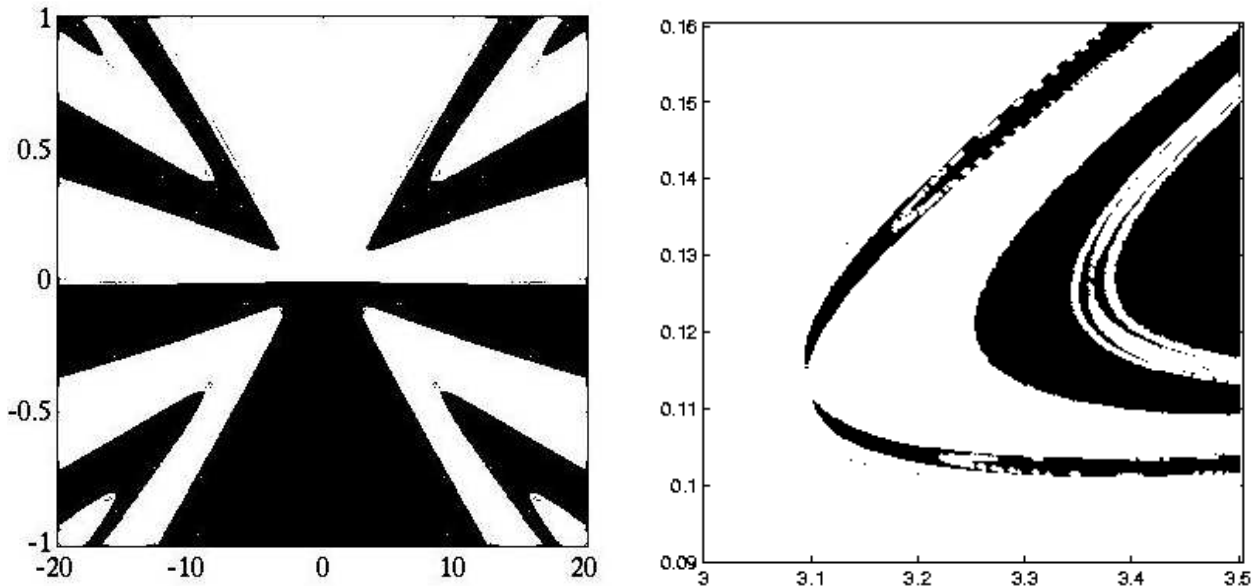


Figure 2. A $\mathbf{u} = 0$ section of phase space for $D = 5$, $N = 2$ timelike trajectories. The points here are colored according to their final outcome. Here and in Figure 5, the second plots show the fractal structure for a small region of the first pictures. Note also that in both figures the horizontal and the vertical axes correspond to the x^1 and x^2 axes, respectively.

d_B . Also, increasing the spacetime dimension makes it more difficult to analyse the fractal structure of the boundaries, the size of the relevant phase space regions generally decreasing with D .

Holographic screens— An interesting physical question is how these features will reflect on the properties of a screen map of the multi-black hole system. The notion of screen mapping was introduced by Susskind in Ref. [13] for $D = 4$ asymptotically flat spacetimes, in an attempt to implement ‘t Hooft’s holographic hypothesis [14]. In this approach, all points of space are mapped by light rays that impinge perpendicularly onto a flat two-dimensional screen in a distant asymptotically flat region. According to the holographic hypothesis, the black hole has the maximal bit density of one per unit area. Thus the horizons of any black holes are necessarily mapped onto sets of larger area on the screen. Corley and Jacobson refined the idea of Susskind and clarified the global properties of such maps [15]. This concept has proven seminal for further developments in the area of the holographic principle [16], [17], [18].

The properties of the screen map of a single black hole have been discussed in [15]. Ref. [19] dealt with two Schwarzschild black holes in the limit of large separation, in which case some of the interesting features of the geodesic motion present in the MP case are absent (also, this configuration presents singularities on the axis joining the black holes [20, 21]).

Following [13], we have considered future directed light rays orthogonally to a screen placed at some distance L from the origin (with L between 10 and 10^3). (Here we will restrict to the case $D = 4$, $N = 2$ and note $x^1 = x$, $x^2 = y$, $x^3 = z$. The black holes are located at ± 1 on the y -axis and have equal masses $M_i = 1/3$, the configuration presenting

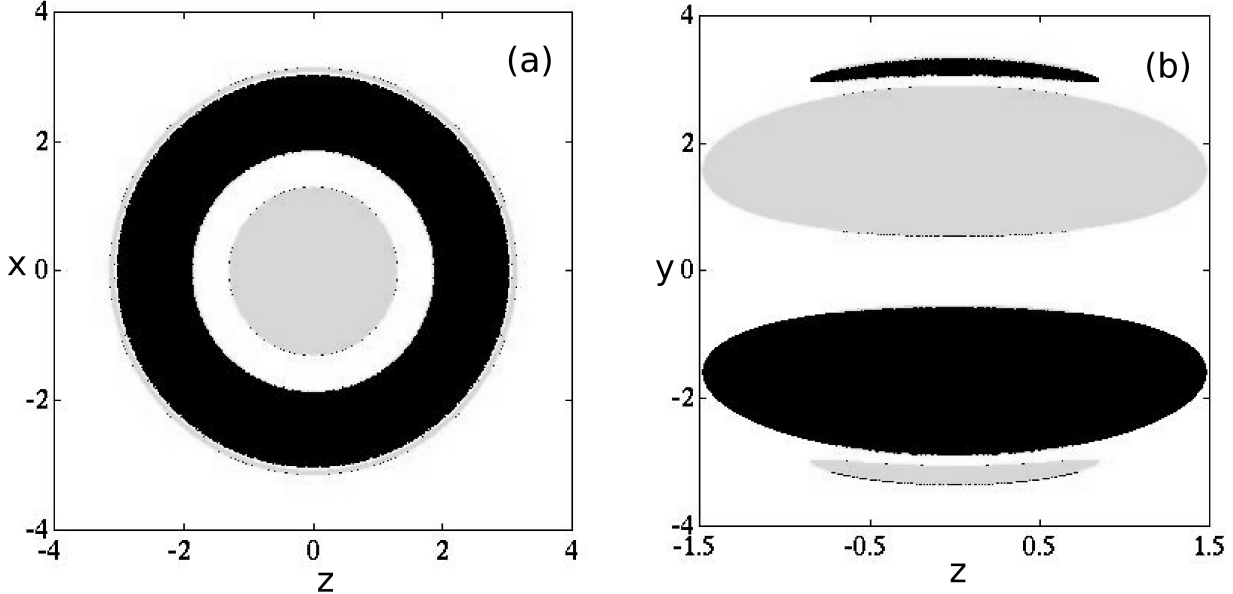


Figure 3. Screen images of a $D = 4$, $N = 2$ system with $M_i = 1/3$. The first black hole is located at $(0, -1, 0)$ and the second one at $(0, 1, 0)$. The screen is placed at $L = 100$, the light rays being perpendicular to the screen with $|\mathbf{u}^{(0)}|=10$. In these pictures, black stays for a particle being captured by the first black hole, gray for the second one and white for particles which orbit indefinitely.

an azimuthal symmetry). The black holes image on the screen depends on the angular location of the screen with respect to the axis joining the black holes. However, we have found that, for any screen location, the black holes have distinct images. For a screen which lies perpendicular to the y -axis (Figure 3a), the image of the second black hole forms a ring around the first. Apart from these primary images, there is also a sequence of concentric rings with decreasing area. The primary black hole images on a screen perpendicular to the x -axis are deformed disks (Figure 3b). Secondary images are found at the y -extremities of these disks. The primary map of an individual black hole has an area which is greater than the horizon area, which gives an entropy density on the screen less than $1/4G$, as expected [13].

In both cases above, zooming the boundary between the region with different outcomes on the screen map reveals a complicated structure, and we notice the existence of a (presumably-) infinite sequence of images with decreasing area.

To understand some of these features, one should remark that the generic picture presented in Figure 2 remains the same for very large values of the radial coordinate. In particular, it appears that the fractal boundary there (and the corresponding one for null motion) continues to spacelike infinity. Also, the data on a planar screen represents a slice of the bulk phase space.

A crucial point here is the observation that when cutting a fractal structure in a plane with a one dimensional line, self-similarity implies that the fractal dust on that line has a fractal dimension $d_B - 1$ [12]. For example, as seen in Figure 4, a fractal structure is induced on a circle of radius r_0 in the (x, y) -plane (with r_0 much greater than the distance between

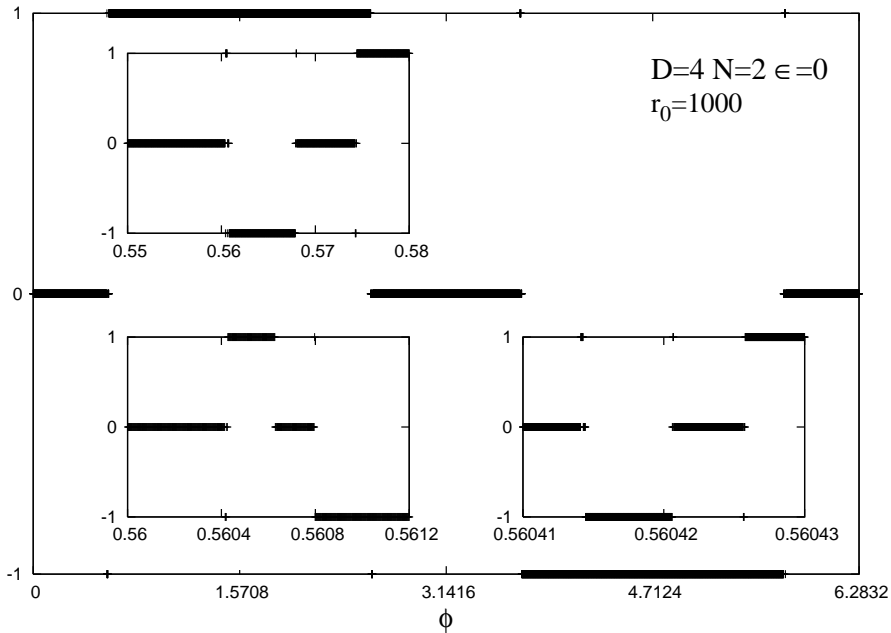


Figure 4. The fractal structure induced on a circle of radius r_0 . ϕ is the coordinate on the circle in the (x, y) -plane, with $\phi = 0$ corresponding to $x = 0$. The vertical axis shows the outcome of the test particles, -1 for the black hole at $(0, -1)$, -1 for the black hole at $(0, 1)$ and 0 for those particles which orbit indefinitely. In the close up views, we show transition regions between various outcomes, each successive view resolving a portion of the previous close up.

the black holes). The photons start orthogonally to the circle, $|\mathbf{u}^{(0)}| = 10$, directed inwards. Zooming a transition region in that plot reveals a self similar structure; the fractal structure was tracked over 12 decades in magnitude before saturating the machine precision.

Since a planar screen can be considered as a portion of a large sphere, this implies the existence of a fractal structure on the planar screen too. Thus, an angular slice along some direction on the screen plane reveals the existence of a self similar structure with a fractal dimension $d_B - 1$, as illustrated in Figure 4.

It is tempting to interpret this feature as a consequence of the holographic principle; studying the black hole images on some screen provides information on the phase structure of the bulk spacetime.

Although we restricted ourselves here to the $D = 4$ case, it is likely that this is a generic property of the geodesic motion in a MP spacetime for any spacetime dimension. Similar results have been found for $D = 5$, $N = 2$ configurations.

Further remarks– The investigation of the geodesics in a higher dimensional MP multi-black hole spacetime revealed that the features of the four dimensional case appear to be generic, the boundary separating in phase space the different asymptotic behaviours being fractal. As usual, the presence of a fractal boundary indicates that there are nonsmooth structures in phase space, which implies that the system is chaotic.

The analysis in this paper can be straightforwardly extended to test particles with an $U(1)$ electric charge q and mass m . We expect that similar to the situation in $D = 4$, the structure of the phase space will depend only slightly on the particle charge, except for the extremal case $q = m$.

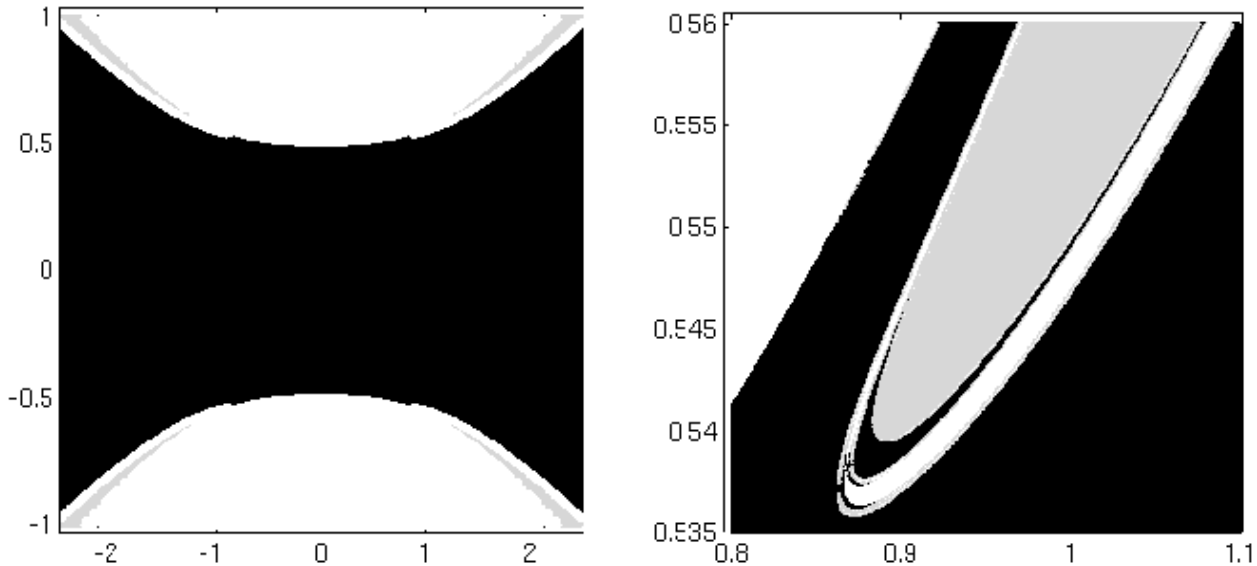


Figure 5. A $\mathbf{u} = 0$ section of phase space for $D = 5, N = 3$ timelike trajectories. The black holes are located on the x^2 -axis, at ± 1 and 0 respectively, and have $M_i = 0.01$. The basin of attraction of the black hole at $x^2 = -1$ is marked in black, the basin of attraction of the black hole at $x^2 = 1$ is marked in white, while those trajectories ending on the black hole at $x^2 = 0$ are marked in gray.

Concerning the configurations with several black holes, we have found that the $N = 2$ pattern repeats up to the $N = 4$ case, the largest number of black holes we considered.

For the case with several black holes placed on the x^2 -axis, the basin of attraction still has a fractal structure. To illustrate these aspects, we give in Figure 5 the results for timelike motion with $\mathbf{u}^{(0)} = 0$ in a $D = 5, N = 3$ MP spacetime. The points in that grid are again colored according to their final outcome.

It is interesting to note that if we place an infinite number of black holes along a line with each a unit distance apart, the resulting spacetime has a periodicity one along the line. This procedure is equivalent to compactifying one dimension on a torus with period one. The resulting solution describes a Kaluza-Klein extremal black hole, presenting nontrivial dependence on the extra-dimension [22]. Our results suggest that the geodesic motion in this background would also present chaotic features. However, a study of this case requires a separate discussion and is beyond the purposes of this work.

Although further work is clearly necessary, we have pointed out a curious relation between the bulk phase structure and the induced map on a holographic screen placed in the asymptotic region. An observer on the screen would notice a fractal structure of the corresponding phase space, whose fractal dimension is the bulk fractal dimension minus one.

We would like to point out that this appears to be a generic feature of gravity solutions presenting chaotic features, the MP spacetime considered here being only one particular case. A similar approach can be applied to other spacetimes presenting chaotic motion. It would be interesting to further explore the connection between the holographic principle and a fractal structure in the bulk.

Acknowledgements

The authors thank Professor D. M. Heffernan for useful discussions. The work of ER is carried out in the framework of Enterprise–Ireland Basic Science Research Project SC/2003/390 of Enterprise-Ireland.

References

- [1] H. Varvoglis and D. Papadopoulos, *Astron. Astrophys.* **261** (1992) 664.
- [2] V. Karas and D. Vokrouhlický *Gen. Relativ. Gravit.* **24** (1992) 729.
- [3] L. Bombelli and E. Calzetta, *Class. Quant. Grav.* **9** (1992) 2573.
- [4] J. M. Aguirregabiria, *Phys. Lett. A* **224** (1997) 234 [arXiv:gr-qc/9604032].
- [5] Y. Sota, S. Suzuki and K. i. Maeda, *Class. Quant. Grav.* **13** (1996) 1241 [arXiv:gr-qc/9505036].
- [6] S. D. Majumdar, *Phys. Rev.* **72** (1947) 390.
- [7] A. Papaetrou, *Proc. Roy. Irish Acad. (Sect. A)* **51** (1947) 191.
- [8] G. Contopoulos, *Proc. R. Soc. London A* **431** (1990) 183;
G. Contopoulos, *Proc. R. Soc. London A* **435** (1991) 551.
- [9] C. P. Dettmann, N. E. Frankel and N. J. Cornish, *Phys. Rev. D* **50** (1994) 618 [arXiv:gr-qc/9402027].
- [10] C. P. Dettmann, N. E. Frankel and N. J. Cornish, *Fractals* **3** (1995) 161 [arXiv:gr-qc/9502014].
- [11] N. J. Cornish and G. W. Gibbons, *Class. Quant. Grav.* **14** (1997) 1865 [arXiv:gr-qc/9612060].
- [12] B. B. Mandelbrot, *“The fractal geometry of nature”*, Freeman, New York (1977).
- [13] L. Susskind, *J. Math. Phys.* **36** (1995) 6377 [arXiv:hep-th/9409089].
- [14] G. ’t Hooft, arXiv:gr-qc/9310026.
- [15] S. Corley and T. Jacobson, *Phys. Rev. D* **53** (1996) 6720 [arXiv:gr-qc/9602043].
- [16] D. Bigatti and L. Susskind, arXiv:hep-th/0002044.
- [17] R. Bousso, *JHEP* **9906** (1999) 028 [arXiv:hep-th/9906022].
- [18] E. K. Boyda, S. Ganguli, P. Horava and U. Varadarajan, *Phys. Rev. D* **67** (2003) 106003 [arXiv:hep-th/0212087].
- [19] M. G. Jackson, *Phys. Rev. D* **64** (2001) 044020 [arXiv:gr-qc/0103078].
- [20] W. Israel and K. A. Khan, *Nuovo Cim.* **33** (1964) 331.
- [21] R. Emparan and E. Teo, *Nucl. Phys. B* **610** (2001) 190 [arXiv:hep-th/0104206].
- [22] R. C. Myers, *Phys. Rev. D* **35** (1987) 455.